PSFC/JA-11-25

Ohmic Energy Confinement Saturation and Core Toroidal Rotation Reversal in Alcator C-Mod Plasmas

Rice,J.E., Greenwald,M.J., Podpaly,Y.A., Reinke,M.L.,
Diamond,P.H.*, Hughes,J.W., Howard,N.T., Ma,Y., Cziegler,I.,
Duval,B.P.**, Ennever,P.C., Ernst,D., Fiore,C.L., Gao,C.,
Irby,J.H., Marmar,E.S., Porkolab,M., Tsujii,N., Wolfe,S.M.

* UCSD
** CRPP EPFL

November 2011

**Plasma Science and Fusion Center
Massachusetts Institute of Technology
Cambridge MA 02139 USA**

Ohmic Energy Confinement Saturation and Core Toroidal Rotation Reversal in Alcator C-Mod Plasmas

J.E. Rice, M.J. Greenwald, Y.A. Podpaly, M.L. Reinke, P.H. Diamond[♯], J.W. Hughes, N.T. Howard,
Y. Ma, I. Cziegler, B.P. Duval[†], P.C. Ennever, D. Ernst, C.L. Fiore, C. Gao, J.H. Irby,
E.S. Marmar, M. Porkolab, N. Tsujii and S.M. Wolfe

Plasma Science and Fusion Center, MIT, Cambridge, MA, USA

[♯]*UCSD, La Jolla, CA, USA*

[†]*CRPP, EPFL, Lausanne, Switzerland*

Abstract

Ohmic energy confinement saturation is found to be closely related to core toroidal rotation reversals in Alcator C-Mod tokamak plasmas. Rotation reversals occur at a critical density, depending on the plasma current and toroidal magnetic field, which coincides with the density separating the linear Ohmic confinement regime from the saturated Ohmic confinement regime. The rotation is directed co-current at low density and abruptly changes direction to counter-current when the energy confinement saturates as the density is increased. Since there is a bifurcation in the direction of the rotation at this critical density, toroidal rotation reversal is a very sensitive indicator in the determination of the regime change. The reversal and confinement saturation results can be unified since these processes occur at a particular value of the collisionality.

1

I. Introduction

It has been widely observed that Ohmic energy confinement in tokamaks increases linearly with electron density, and then saturates at a critical density [1, 2, 3, 4, 5, 6, 7, 8, 9, 10, 11, 12, 13, 14, 15]. An example of this behavior is shown in Fig.1, which
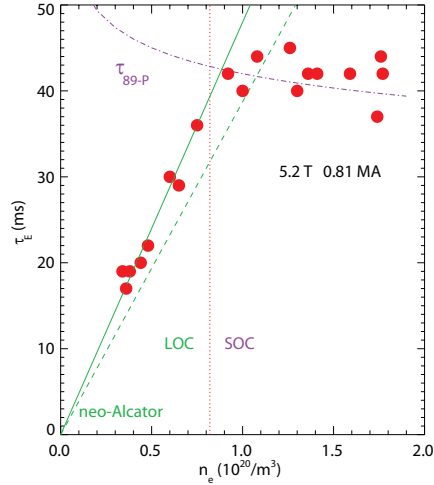

Figure 1: The energy confinement time (from kinetic profiles) as a function of average electron density for a series of 5.2 T, 0.81 MA Ohmic discharges. The dotted vertical line indicates the boundary between the LOC and SOC regimes. The dashed line is the neo-Alcator scaling, the solid line is the best fit to the low density points and the dash-dot line is the ITER-89P L-mode scaling.

was obtained from a shot by shot scan of the electron density in 5.2 T, 0.81 MA (q_{95} = 4.3) plasmas from Alcator C-Mod [13]. The energy confinement time was determined from the kinetic profiles during the steady state portion of each discharge. The vertical dotted line indicates the separation between the linear Ohmic confinement (LOC) and saturated Ohmic confinement (SOC) regimes, at a line-averaged electron density around $0.8 \times 10^{20}/m^3$ for these conditions. The dashed line represents the neo-Alcator scaling [16], $\tau_{nA}(ms) = 70 \, n_e \, q \, \sqrt{\kappa} \, a \, R^2$, with a and R in m and n_e in $10^{20}/m^3$. This line is fairly close to the low density data points. For these discharges, the elongation,

κ, was 1.6, with a = 0.22 m and R = 0.68 m. This particular scaling was developed for circular plasmas (with an *ad hoc* $\sqrt{\kappa}$ added) and doesn't include contemporary devices. For comparison, the solid line indicates the best linear fit to the low density points. At high density, in the saturated regime, the data points are well represented by the ITER-89P L-mode confinement time scaling [17], τ_{89P} (ms) = 48 $I^{0.85}$ $R^{1.2}$ $a^{0.3}$ $\kappa^{0.5}$ $B^{0.2}$ $A^{0.5}$ $n_e^{-0.1}$ $P^{-0.5}$ (with I in MA, B in T and A, the atomic mass of the background ion, in AMU), shown by the dash-dot line. For these deuterium discharges the Ohmic input power, P, was around 0.9 MW, and the agreement between the scaling and the observations is quite good.

The behavior in the LOC regime is not well understood theoretically. The commonly accepted *ansatz* is that at low density, electron turbulence regulates the confinement, while in the saturated regime, ion temperature gradient (ITG) modes dominate [8, 11, 18]. In fact measured turbulence changes at the LOC/SOC transition are in agreement with this concept [19, 20, 11, 21, 14, 15]. It should be noted that this transition is somewhat abrupt. Following the discovery of H-mode, very little effort has gone into the understanding of these Ohmic confinement regimes. The recent results associating Ohmic energy confinement saturation with core toroidal rotation reversals [14, 15] have shed new light on this old problem.

The outline of this paper is as follows: the experimental setup is briefly described in section II. The connection between the LOC/SOC transition and core toroidal rotation reversals, unification of observations with collisionality and a comparison of results from many different devices is shown in section III. Additional rotation reversal observations is presented in section IV, followed by discussion, including the results from gyro-kinetic code simulations, and conclusions in section V.

II. Experimental Setup

These experiments were performed on the Alcator C-Mod tokamak [22], a compact (R_0 = 0.67 m, a $\sim$ 0.21 m), high magnetic field (B $\leq$ 8 T) device with strong shaping capabilities. For the observations presented here, the plasma current was in the range from 0.4 to 1.2 MA, the toroidal magnetic field was between 2.8 and 8 T and the elongation ranged from 1.5 to 1.7. Systematic density scans were performed shot by shot from 0.3 to 2.0×10^{20}/m^3. Electron density and temperature profiles were measured using Thomson scattering [23], Z_{eff} was determined from visible *bremsstrahlung* [23] and core toroidal rotation and ion temperatures were measured with a high resolution imaging x-ray spectrometer system [24]. The energy confinement time was evaluated both from magnetics measurements [23] and from complete density and temperature profiles. All observations presented here were from diverted Ohmic L-mode plasmas, and the results are all averaged over sawtooth oscillations.

III. Ohmic Confinement Saturation and Rotation Reversals

The correlation between the LOC/SOC transition and rotation reversals is demon-

strated in Fig.2, from electron density scans at 5.2 T, for two different plasma currents. For 0.62 MA discharges (q_{95}=5.0), the critical density for rotation reversal was
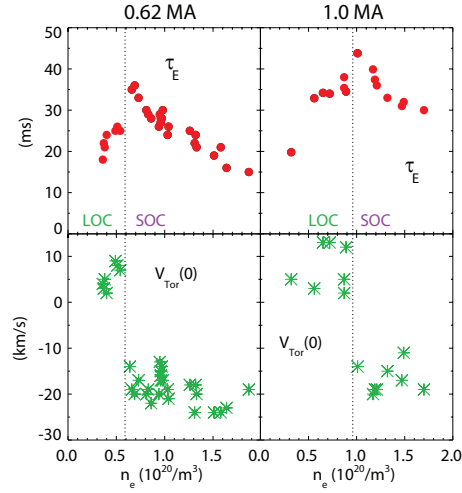

Figure 2: The energy confinement times from magnetics (top) and the core toroidal rotation velocities (bottom) as a function of line averaged electron density for 5.2 T discharges with plasma currents of 0.62 MA (left) and 1.0 MA (right). The vertical dashed lines indicate the locations of the co- to counter-current rotation and LOC/SOC boundaries.

0.59×10^{20}/m^3 (bottom left), very close to the break in slope of the energy confinement time [14, 15] (top left). Below this density the rotation is directed co-current while above the threshold the rotation is in the counter-current direction (indicated by negative values). Here the confinement time was determined from magnetics measurements since full kinetic profiles were not available for all of the discharges. For the 1.0 MA plasmas (q_{95}=3.2), the density for rotation reversal (bottom right) and confinement saturation (top right) also coincide, but in this case at 0.96×10^{20}/m^3. From a series of density scans at different plasma currents and fixed magnetic field (5.2 T), the LOC/SOC transition density has been determined (from shot by shot density scans of the energy confinement time) as a function of I_p, and is shown in the top panel of Fig.3. This linear increase of the confinement saturation density with plasma current has also
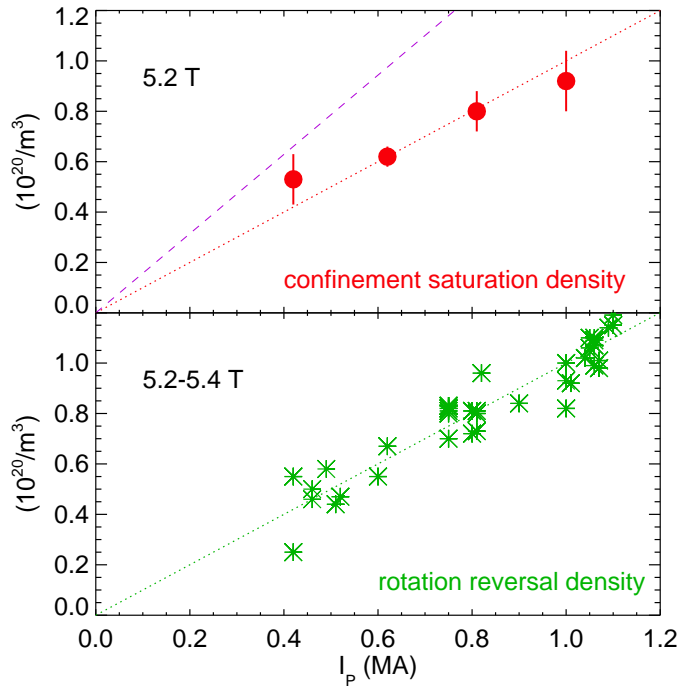
Figure 3: The transition density between the LOC and SOC regimes (top) and the critical density for core toroidal rotation reversals (bottom) as a function of plasma current for fixed magnetic field. The dotted lines have the same slope. The dashed line is an empirical scaling [3].

been observed in JFT-2M discharges [3]. The dashed curve represents an empirical scaling, $n_{crit} = 0.65 \sqrt{A}$ B/R q [3], derived from four JAERI tokamaks. Shown for comparison in the bottom panel of Fig.3 is the rotation reversal density, which has the same dependence (and slope) as for the confinement saturation [14, 15], indicating the close relationship between the two phenomena. The dotted line in the botom frame is the best fit to the data points; the dotted line in the top frame is the same line as shown in the bottom frame. There are many more points for the rotation reversals, since the critical density can be determined in a single discharge from a slight density ramp, and a change in sign of the rotation velocity is quite easy to detect [25, 26, 27, 14, 15]. To find the confinement saturation density, a complete shot by shot density scan is required, which can take the better part of a single run day. Also, the exact density where the change in slope of the energy confinement time between LOC and SOC occurs is not as precise as the reversal density (see Figs.1 and 2).

Shot by shot scans of other relevant parameters, the electron and ion temperatures, Z_{eff} and R/L_n (evaluated at r/a = 0.6), for the 0.62 MA, 5.2 T discharges of Fig.2 are shown in Fig.4. The temperatures and Z_{eff} vary monotonically with density. At the LOC/SOC transition, the value of T_e/T_i was ~1.35 [14]; this is close to T_e/T_i ~1.5 observed in ASDEX Upgrade at the LOC/SOC transition [18]. In contrast, there is an abrupt change in slope of the density gradient scale length (bottom frame) at the transition density. In the LOC regime, as the density increases, the electron density profile becomes more peaked. In the saturated regime, the density profile maintains its shape. Similar behavior has been observed in ASDEX Upgrade plasmas as well [18]; at the LOC-SOC transition the value of R/L_n at the mid radius was ~5.5, the same as for C-Mod in Fig.4.

In an attempt to unify the rotation reversal and confinement saturation observations, and in order to understand why the processes occur at a different electron density for different plasma currents, the collisionality has been examined. Shown in Fig.5 are the central rotation velocities as a function of effective collisionality in the core for the density scans at 0.62 and 1.0 MA. Here ν_{eff} is the ratio between the collision frequency and the curvature drift frequency, given by $\nu_{eff} \approx R\ Z_{eff}\ n_e/T_e{}^2$, with R in m, n_e in $10^{20}/m^3$ and T_e in keV. The reversals occur for similar values of ν_{eff}, 0.32 for the lower current and 0.42 for the higher current plasmas. These numbers are somewhat similar in magnitude to $\nu_{eff} = 0.9$ where the turbulence propagation (measured by Doppler reflectometry) changed sign in ASDEX Upgrade plasmas [21]. The rotation reversals also coincide (for the same scans) using the collisionality ν_*, the ratio of collision frequency to the bounce frequency ($\nu_* \equiv 0.0118\ q\ R\ Z_{eff}\ n_e/T_e{}^2\ \epsilon^{1.5}$) as shown in Fig.6. For this plot, ν_* was evaluated at the q=3/2 surface, which is the radius inside of which the rotation reversal occurs [14]. For the 0.62 MA and 1.0 MA discharges, the q=3/2 surfaces were located at r/a $\sim$ 0.5 and 0.7, respectively. In this case the ν_* values for the reversals are very close, 0.41 for 0.62 MA and 0.45 for 1.0 MA. This agreement may be fortuitous since ν_* is very sensitive to the electron temperature; at other radial locations the agreement may not be so good. These values are also very close to the number $\nu_* = 0.35$ evaluated at r/a=0.7, where the turbulence propagation reversals were observed at ASDEX Upgrade [21].

Since the density for rotation reversal and confinement saturation is proportional to plasma current ($n_{crit} \propto I_p \propto q^{-1}$), it's not surprising that this occurs at $\nu_* \propto nq = const.$
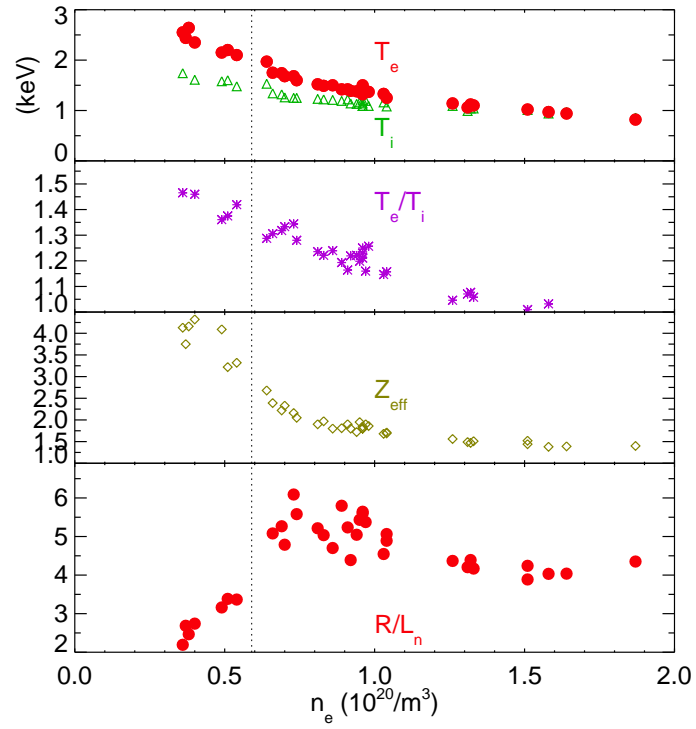
6

Figure 4: The electron and ion temperatures (top), their ratio (second frame), effective Z (third frame) and inverse density gradient scale length at r/a = 0.6 (bottom) as a function of electron density for 0.62 MA, 5.2 T discharges. The dotted vertical line indicates the LOC/SOC transition density.
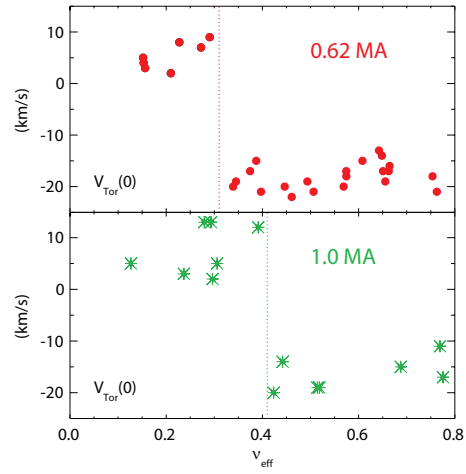
7

Figure 5: The core toroidal rotation velocities as a function of ν_{eff} for plasma currents of 0.62 MA (top) and 1.0 MA (bottom). Vertical lines indicate the co- to counter-current rotation boundary.
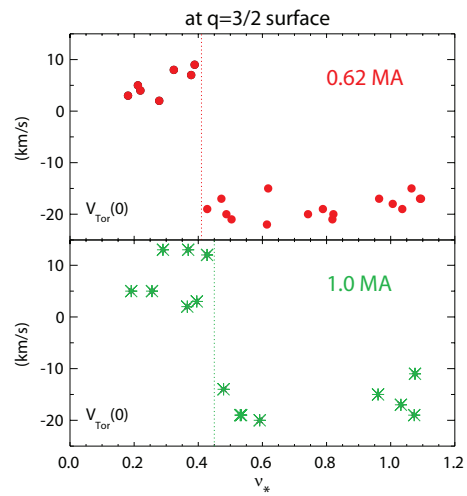
Figure 6: The core toroidal rotation velocities as a function of ν_* for plasma currents of 0.62 MA (top) and 1.0 MA (bottom). Vertical lines indicate the co- to counter-current rotation boundary.

This speculation can be further supported by comparing confinement saturation results from several devices referenced in the Introduction. Shown in Fig.7 is the density of the LOC/SOC transition at fixed q (between 2.8 and 3.8) as a function of major radius for various tokamaks. These results are consistent with a 1/R scaling. The point from TCV
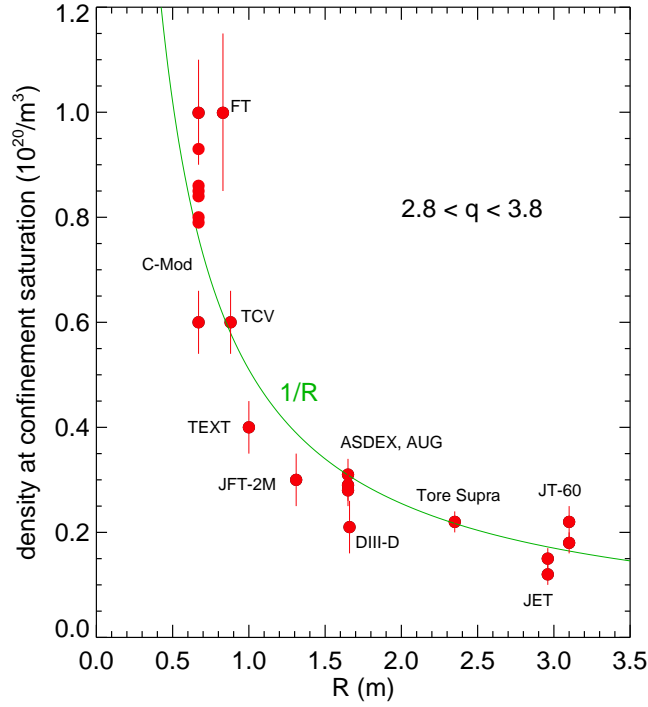

Figure 7: The transition density from LOC to SOC as a function of major radius for different devices at fixed values of q. The solid curve represents 1/R.

[25] and those from C-Mod without error bars are from rotation reversals. For ITER plasmas, the boundary density between LOC and SOC is expected to be $\leq 1 \times 10^{19}/m^3$, based on an extrapolation of Fig.7. These results suggest that confinement saturation may occur at a fixed value of collisionality, with $\nu_* \propto nRq = const$. The C-Mod and AUG results are consistent with a value $\nu_* \simeq 0.4$ for $r/a \sim 0.7$.

There is a factor of Z_{eff}/T_e^2 in the expressions for the collisionality. It turns out that this is a weakly varying function of density near the transition point, as can be seen in Fig.8, which was derived from Fig.4. The ratio is about 0.8 at the revesal density, and only changes by $\sim 20\%$ over this density range, thus contributing to the collisionality variation only slightly.
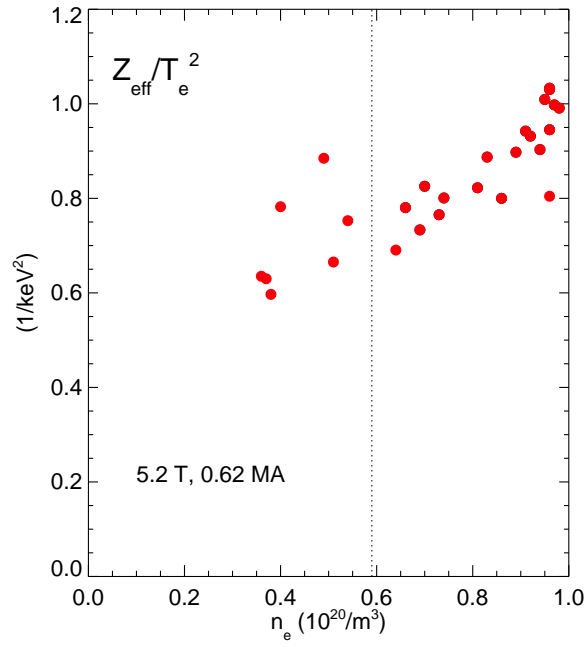
Figure 8: The ratio Z_{eff}/T_e^2 as a function of density for the 5.2 T, 0.62 MA discharges of Fig.4, in the vicinity of the LOC-SOC transition point.

IV. Rotation Reversal Characteristics

In the previous section, rotation reversals were obtained by changing the electron density, either by means of dynamic ramps or during shot to shot scans. Reversals can also be induced by changing the plasma current, as is demonstrated in Fig.9. The plasma current was ramped down in steps for this 6.3 T discharge, while the density was held fixed. As the plasma current was reduced, the rotation reversed direction and
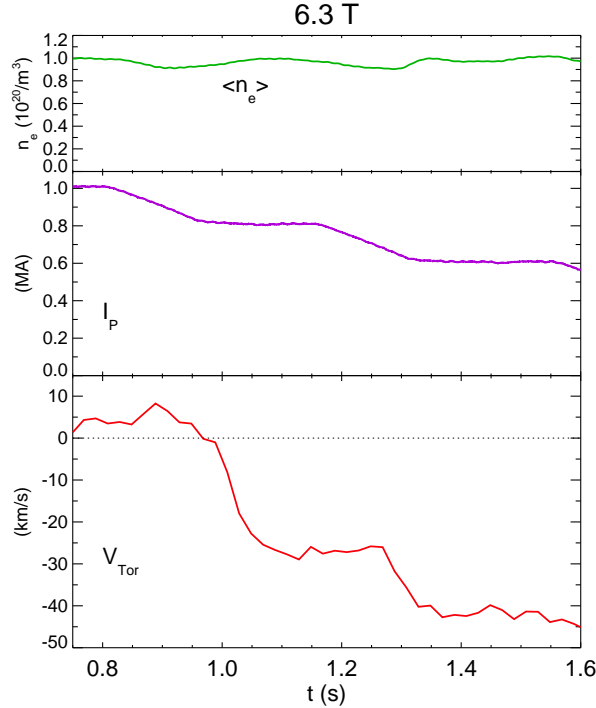

Figure 9: The electron density (top), plasma current (middle) and core rotation velocity (bottom) for a 6.3 T discharge with downward current ramps.

incremented in the counter-current direction. There was a delay in the response of the rotation to the current ramps. This delay is between the momentum confinement time ($\sim$30ms) [28] and the current relaxation time. The dependence of the core toroidal rotation velocity on plasma current is shown in Fig.10, from a shot by shot scan at fixed magnetic field (5.2 T) and electron density (0.8-$1.2\times10^{20}/m^3$). There is a linear increase in the velocity with plasma current [29, 30], trending in the co-current direction. The velocity reverses direction at around 0.9 MA for this range of density, consistent with the density ramp results at fixed current [14]. This trend with plasma current in L-mode plasmas is the inverse of the current dependence in H-mode, I-mode and other enhanced confinement regimes, where the toroidal rotation velocity was found to scale $\propto 1/I_P$ [31, 32, 33].

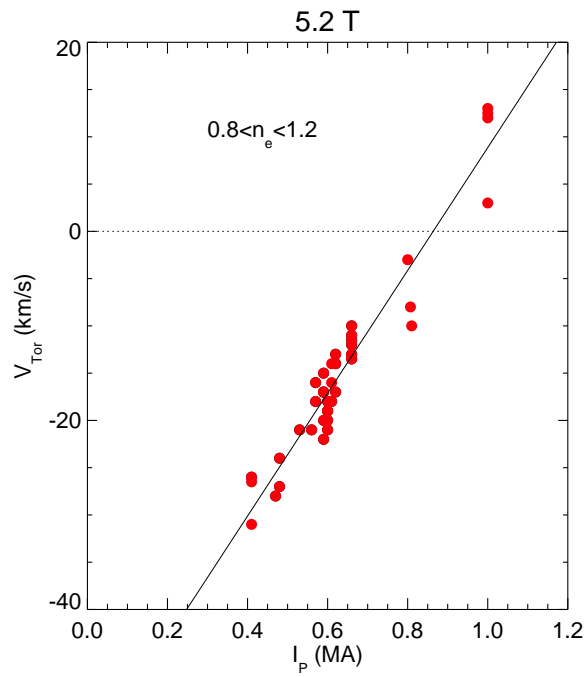Rotation reversals have also been observed with magnetic field ramps at fixed den-

Figure 10: The core rotation velocity as a function of plasma current at fixed magnetic field and electron density. The solid line is the best linear fit.

sity [14]. Shown in Fig.11 are the parameter time histories in a 0.8 MA discharge with a downward magnetic field ramp. As the magnetic field was decreased, the core
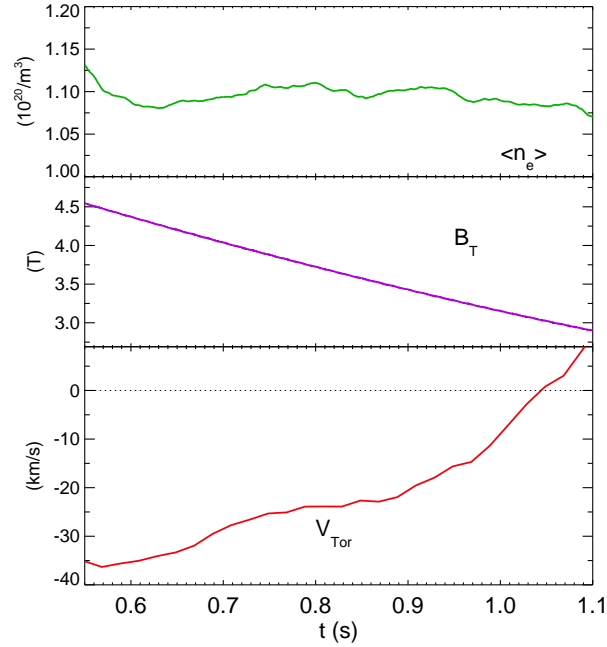

Figure 11: Time histories of the electron density (top), toroidal magnetic field (middle) and core rotation velocity (bottom) in a 0.8 MA plasma with a downward magnetic field ramp.

toroidal rotation velocity incremented in the co-current direction and eventually reversed. In general, with increasing magnetic field, the rotation velocity becomes more counter-current [29, 34]. Shown in Fig.12 is the core rotation velocity as a function of magnetic field at fixed plasma current (1.0 MA) and electron density ($1.17 \times 10^{20}/m^3$) from a shot by shot scan. Although the rotation velocity did not reverse in this scan, it would be expected to change direction around 6 T, consistent with other observations [14]. Unlike the density dependence, where an abrupt rotation reversal is seen for a small change in n_e, there is a continuous dependence on plasma current and magnetic field at fixed density, with weaker bifurcation. This may explain the lack of hysteresis seen with magnetic field ramps [14]. Regardless of the dynamics, these trends with plasma current and magnetic field are consistent with the notion that reversals occur at fixed collisionality, with $\nu_* \propto nq = \text{const}$.

An important clue to the underlying cause for the rotation reversals and the LOC-SOC transition can be found by examining associated changes in the core turbulence characteristics. At low density, in the LOC regime, a feature in the spectra of density fluctuations (measured with the phase contrast imaging diagnostic) extending up to and
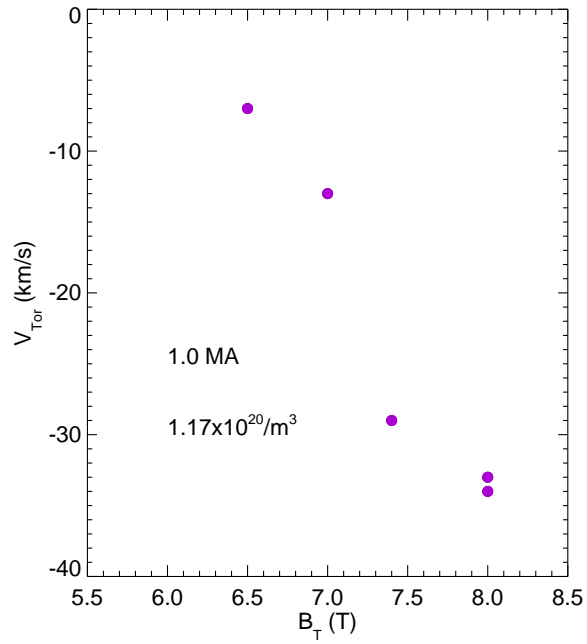
14

Figure 12: The core toroidal rotation velocity as a function of toroidal magnetic field at fixed plasma current and electron density.

above $k_\theta \sim 10$ cm^{-1} is present [14, 15], which disappears abruptly as the density is raised and the rotation reverses direction. An example of the fluctuation spectrum S(k,f) for a 5.2 T, 1.0 MA discharge is shown in Fig.13. This dispersion plot is the difference
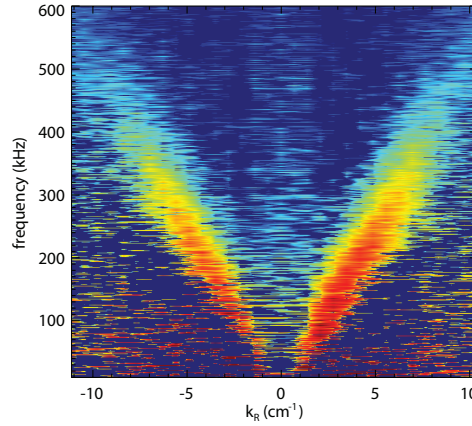

Figure 13: The density fluctuation spectrum S(k,f) of the difference between dispersion plots taken at two times during a 5.2 T, 1.0 MA discharge.

between spectra obtained at electron densities of 0.98×10^{20}/m^3 (co-current rotation, LOC regime) and 1.07×10^{20}/m^3 (counter-current rotation, SOC regime). These density fluctuations from the core of the plasma, which are only present below the critical reversal density (LOC regime), have k_θ between 2 and 11 cm^{-1} and $k_\theta \rho_s$ between 0.15 and 0.7, consistent in nature with trapped electron modes (TEMs) [15], at least for the higher k values. The slope of the features in Fig.13 indicates a phase velocity of around 3 km/s.

V. Discussion and Conclusions

The connection among rotation reversals, the transition between the LOC and SOC regimes and changes in turbulence is well established. These observations can be uni-

fied with the following *ansatz* [35]: at low collisionality, the core toroidal rotation is directed co-current, the turbulence is dominated by TEMs, and Ohmic energy confinement and density profile peaking increase with increasing collisionality. At a critical value of the collisionality ($\nu_* \sim 0.4$), the density profile peaking stops, TEMs abruptly disappear, ion temperature gradient (ITG) modes dominate, the rotation switches to the counter-current direction and Ohmic energy confinement saturates. Unfortunately for the present observations, there are no direct measurements verifying the dominance of ITG modes at high densities following the reversal.

In order to test this concept, simulations have been performed using the gyrokinetic code GYRO [36]. Shown in Fig.14 are contour plots of the linear growth rates of the most unstable modes with $0.25 < k_\theta \rho_s < 0.75$ in the a/L_n-a/L_T plane. The solid lines going from the bottom left to top right in both figures separate the regions of TEM and ITG dominance. Depicted by the $+$ in the plot on the right is the operational point
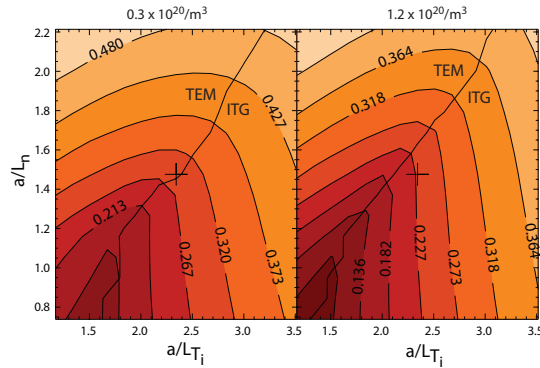

Figure 14: Contour plots of the linear growth rates (in units of c_s/a) of the most unstable modes (with $0.25 < k_\theta \rho_s < 0.75$) in the a/L_n-a/L_T plane. The $+$ signs indicate the location of discharges with $n_e = 0.3 \times 10^{20}/m^3$ (left) and $1.2 \times 10^{20}/m^3$ (right).

for a 0.62 MA discharge ($q_{95} = 5.6$) with an electron density of $1.2 \times 10^{20}/m^3$, which indicates that the most unstable mode is ITG. Lowering the density (collisionality) a

factor of 4 moves the operational point to the TEM branch, as shown on the left. This is in qualitative agreement with the observations and the scenario described above.

Some open questions which remain regard why the LOC/SOC transition appears to occur near $\nu_* = 0.4$ and for $T_e/T_i \sim 1.4$.

In summary, the close connection between rotation reversal and Ohmic energy confinement saturation has been demonstrated. Concomitant changes in the nature of density fluctuations and electron density profile peaking are also observed. These phenomena occur at a very specific value of the electron density, which increases with plasma current. A comparison of Ohmic confinement saturation on a large number of devices indicates that this critial density scales with the inverse of the device major radius. The last two points suggest that these processes occur at a fixed value of the collisionality.

VI. Acknowledgements

References

[1] R.R.Parker et al., Nucl. Fusion **25** (1985) 1127.

[2] R.V.Bravenec et al., Plasma Phys. Contr. Fusion **27** (1985) 1335.

[3] Y.Shimomura et al., 'Empirical Scaling of Energy Confinement Time of L-Mode and Optimized Mode and Some Consideration of Reactor Core Plasma in Toka-mak' JAERI Report 87-080 (1987)

[4] S.Sengoku et al., J. Nucl. Materials **145-147** (1987) 556.

[5] F.X.Söldner et al., Phys. Rev. Lett. **61** (1988) 1105.

[6] F.Alladio et al., Plasma Physics and Controlled Nuclear Fusion Research Proc. 13th Int. Conf. 1990 (Washington) Vol. 1 (Vienna: IAEA) p.153.

[7] X.Garbet et al., Controlled Fusion and Plasma Physics, Proc. 19th European Conf. (Innsbruck, 1992) Vol. 16C p.107.

[8] F.Wagner et al., Plasma Phys. Contr. Fusion **35** (1993) 1321.

[9] F.Ryter et al., Plasma Phys. Contr. Fusion **36** (1994) A99.

[10] G.Bracco et al., Nucl. Fusion **37** (1997) 759.

[11] C.L.Rettig et al., Phys. Plasmas **8** (2001) 2232.

[12] M.Greenwald et al., Fusion Sci. Technol. **51** (2007) 266.

[13] L.Lin et al., Plasma Phys. Contr. Fusion **51** (2009) 065006.

[14] J.E.Rice et al., Nucl. Fusion **51** (2011) 083005.

[15] J.E.Rice et al., submitted to Phys. Rev. Lett. (2011)

[16] R.J.Goldston, Plasma Phys. Contr. Fusion **26** (1984) 87.

[17] P.N.Yushmanov et al., Nucl. Fusion **30** (1990) 1999.

[18] C.Angioni et al., Phys. Plasmas **12** (2005) 040701.

[19] R.L.Watterson et al., Phys. Fluids **28** (1985) 2857.

[20] D.L.Brower et al., Phys. Rev. Lett. **59** (1987) 48.

[21] G.D.Conway et al., Nucl. Fusion **46** (2006) S799.

[22] E.S.Marmar et al., Fusion Sci. Technol. **51** (2007) 261.

[23] N.P.Basse et al., Fusion Sci. Technol. **51** (2007) 476.

[24] A.Ince-Cushman et al., Rev. Sci. Instrum. **79**(2008) 10E302.

[25] A.Bortolon et al., Phys. Rev. Lett. **97** (2006) 235003.

[26] B.P.Duval et al., Plasma Phys. Contr. Fusion **49** (2007) B195.

[27] B.P.Duval et al., Phys. Plasmas **15** (2008) 056113.

[28] J.E.Rice et al., Nucl. Fusion **44** (2004) 379.

[29] J.E.Rice et al., Nucl. Fusion **45** (2005) 251.

[30] L.-G.Eriksson et al., Plasma Phys. Contr. Fusion **51** (2009) 044008.

[31] J.E.Rice et al., Nucl. Fusion **39** (1999) 1175.

[32] J.E.Rice et al., Nucl. Fusion **47** (2007) 1618.

[33] J.E.Rice et al., Phys. Rev. Lett. **106** (2011) 215001.

[34] J.E.Rice et al., Plasma Phys. Contr. Fusion **50** (2008) 124042.

[35] P.H.Diamond et al., Phys. Plasmas **15** (2008) 012303.

[36] J.Candy and R.E.Waltz, J. Comput. Phys. **186** (2003) 545.